 CMC, vol.28, no.3, pp.213-230, 2012

Statistical Analysis of Macromolecular Chains in the Space Filled by Nanoparticles

J. Zidek[1,2], J. Kucera[1] and J. Jancar[1,2]

Abstract: The paper presents a combination of worm-like chain numerical models and one with a finite set of nano-particles. The primary objective of the models was to analyze the distribution of space in a system filled by particles. Information on the distribution of space was compared to properties of chains inside the set of particles. The set of nanoparticles was constructed with a tool generating a finite set of particles that is randomly distributed in a given space. The particles have a prescribed volume fraction and uniform size. First, the proportions of chains and particles were compared. The length of chain was expressed in terms of end-to-end length. It was then compared to the size of gaps between two particles. The volume of chain was compared to the volume of space delimited by the particles. Next, a set of 10,000 random chains was generated and these were introduced into the particle set. The contact of a chain with the surface of a particle resulted in the special structural elements of the chain: a chain connecting two different particles, a loop which begins and ends at the same particle, a part of a chain which is completely adhered to the particle surface, a chain attached to a particle with one free end, as well as completely free chains. The chains were classified under three classes: chains which were not in contact with particles, chains which were in contact with one particle, and chains which were in contact with two or more particles. A statistical representation of each class is presented. The contact between chain and particle can influence macroscopic properties such as those that are elastic.

Keywords: worm-like chain, chain, nanocomposites, microcomposite, Voronoi diagrams

1 Introduction

Numerical models can be applied to the analysis of certain effects whose essence represents the difference between the nano- and micro-structure of composites.

[1] Brno University of Technology, Brno, Czech Republic.
[2] Central European Institute of Technology, Brno, Czech Republic.

Two examples of effects with different nano and microcomposites are discussed in this paper. The first is the impact of some macroscopic properties (mechanical, electrical, transportational) on the size of particles. Up to micrometer particle size, the properties do not depend on a dwindling particle size. From micrometer to nanometer size, the properties' dependence on particle size is very steep. Such a function are mechanical properties [Kalfus and Jancar 2007; Bansal, Yang, Cho, Benicewicz, Kumar, Schadler 2005; Akcora, Liu, Kumar, Moll, Li, Benicewicz, Schadler, Acehin, Panagiotopoulos, Pryamitsyn, Ganesan, Ilavsky, Thiyagarajan, Colby and Douglas 2009], gas permeability [Osman and Atallah 2004], and electrical conductivity [Torquato, Hyun and Donev 2002; Ye, Lai, Liu and Tholen 1999].

Next, the interval of volume fractions, which can effectively improve material properties, is different for micro- and nano-composite. In micro-composites, a significant change in macroscopic properties is observed when the volume fraction is at least 10%. The maximal degree of filling can be up to 50% or more. However, the nano-filler usually shows the effect at much lower concentrations of about 2-5%. The maximum filling is about 15-20%. A further increase in volume fraction does not have any additional effect, and can even lead to a deterioration in nano-composite qualities.

The different behaviors of nano- and micro- composites are interpreted by the relative size of chain and particle [Jancar, Douglas, Starr, Kumar, Cassagnau, Lesser, Sternstein and Buehler 2010]. In the case of micro-composites, the chain size is much lower than the particle size. The polymer phase, as well as the particle phase, can be considered a continuum. The complex properties of the micro-composite system can be derived from properties of the continuous phase (polymer), the continuous filler phase (particle), and the filler shape phase. These properties can be described by solid phase models. Such models (Finite Element Method) assume that properties are independent of particle size [Agarwall 1972].

The matrix in nano-composites cannot be considered a physical continuum. The chains at molecular levels have an irregular shape and the structure of the volume related to the chains is more complex. The cells of relatively large volume (in the spaces among several particles) are alternated with narrow spaces (between two opposite spherical caps). In such a structured space, the collisions of chains and particles can occur somewhat frequently.

The modeling of nano-composite or micro-composite effects can be performed at different scales. As stated above, from the standpoint of the length scale, the micro-composite is a relatively simple system, which can be described using the Finite Element Method.

The nano-composite material is usually analyzed using molecular models. How-

ever, a representative volume of nano-composite must contain a large number of atoms as the purely atomistic simulations are limited by computer power. The problem is frequently solved by a coarse grain model [Knauert, Douglas and Starr 2007], in which the atoms are substituted by atomic groups. The next approach is to reduce the size of the nano-filler as much as possible. For example, one molecule of silsequioxanes (POSS) can, at the same time, be the smallest nano-particle [Bizet, Galy and Gérard 2006].

The approach applied in this paper is a hybrid one modeling the continual solid phase and a coarse grained molecular approach. The solid phase models can be applied to the modeling of nano-particles. Each particle is a space delimited by the analytical equation of a sphere. The set of non-intersecting spheres was generated using the AGLOMER software [Zidek, Kucera and Jancar 2010]. The AGLOMER software produces a set of random spheres with a given user-defined: 1. volume fraction, 2. particle size distribution, and 3. number of particles. The result from the software is a set of particle coordinates and radii. Particles are closed in a cubic box or in the reference sphere. The generated set is usually composed of between tens of thousands and hundreds of thousands of particles and, in our analysis, its macroscopic homogeneity was tested and proved.

The polymer matrix was modeled as a set of worm-like chains of carbon backbone atoms. The chain was generated by an in-house script [Hynstova, Jancar and Zidek 2006]. The output of the script was a numerical model of the worm-like chain including coordinates of the segments. The worm-like chain is a common model of a macromolecular chain. Its parameters are the length of segment and bond angle (*see Figure 1*). In contrast to the random walk chain, the basic model of a worm-like chain reflects the correct geometrical properties of molecules. The model can be verified by a comparison of the mean quadratic end-to-end length. The parameter can be calculated from the numerical model and expressed analytically. In the simplest modification called a freely rotating chain, the mean quadratic end-to-end length (l) can be calculated from the number of segments (N), the length of segment l_s, and the bond angle (φ):

$$\left\langle l^2 \right\rangle = N \, \frac{1+\cos(\pi-\varphi)}{1-\cos(\pi-\varphi)} \, l_s^2 \tag{1}$$

For this paper, the script generating chains was modified. The additional function of avoiding chains and particles was introduced into the script. Each contact of a chain with a nano-particle was recorded.

The combination of such components can give a picture of the coexistence of nano-particles and macromolecular chains within the same space *(see Figure 1)*. The particles form a restricted space and the filling of the space by the chain is limited

by its geometrical properties.

The numerical model (of a chain in coexistence with particles) contains special structural elements. We sorted the parts of a chain according to the proximity of the chain and particle. The classes of structural elements are shown in *Fig. 1*. A chain which was far from any particle was called a free chain (F). A part of a chain which had one grafted end (G), a part of a chain which completely adhered to a particle surface (A), and loops (L) were frequently observed. The specific component was a connector (C) joining two or more particles together.

Of course, one chain can contain a combination of extra different structural elements, with the exception of a free chain (F). If the chain was of type F, it was excluded by the presence of any other component. However, it was possible to get a chain composed of several loops with adhered and grafted parts. The analysis was complex and very difficult. As such, the situation was simplified into three cases: the free chain (chains exclusively of type F), a chain near the surface of one particle (containing any combination of A, G, L), and a chain connecting two or more particles (containing at least one component C).

Most of the components (G, A, and L) will be observed in both nano- and micro-composites. The nano- and micro-composite differ in their relative representations. It is presumed that most of the chains in micro-composites are far from any particle (type F). The nano-composite contains various representations of structural elements.

It is very important to note that the connectors can only be observed in nano-composites. They are practically absent in micro-composites, because the distance of filler particles is too high in comparison to the length of chains. In nano-composites, where the distance of particles is comparable to the length of chains, the presence of connection components is important.

The geometrical aspects of nano-particles and chains are interpreted by a schematic 2D picture of particles and parts of macromolecules arranged in 2D cells (*see Figure 2 a*). It is useful for the qualitative interpretation of results, but provides no clue over the exact geometrical aspects. The schematic drawing can be confusing in certain respects. First, the interparticle space in 2D schematic drawings is much denser than in real 3D situations.

Second, principally from the 2D scheme, it seems that some chains are in a very small space cell, which is closed due to particle surfaces (marked in *Figure 2* as closed space by an *arrow*).The chains in such a space cannot diffuse into the neighbouring cells. It is inconsistent with reality in 3D. In real 3D structures, the space is less dense than in the 2D schema. Thus, what seems in 2D to be very close contact between two particles is, in 3D space, still a structural component in relatively free

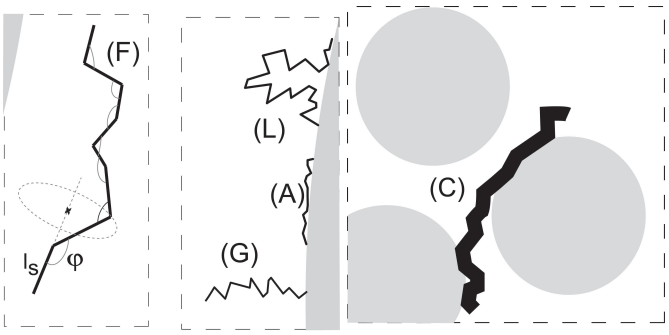

Figure 1: The building of a random worm-like chain (l_s- length of segment; φ – bond angle) into the system of: a. a free chain; b. chains in a microparticle system; and c. nano-particles. Four structural components [free chains (F), grafted chains (G), loops (L), and adhered chains (A)] are observed in both micro- and nano-composites. Connections (C) are observed only in nano-composites.

space. The 3D structure cannot contain the closed spaces. A demonstration of this fact is shown in *Figure 3*. The figure shows the hexagonal close packing distributions of spheres. It is one of two lattices (the second is the face-centered cubic lattice) which allows for maximum possible filling space with 74.048% of the volume of monodispersed spheres. The interparticle phase is continuous even in such a situation and does not contain any closed cells. This is not evident from the picture of spheres alone. Therefore, the channels of interparticle space are highlighted in *Figure 3 (dark gray)*. Such continuous channels form a continuous (without closed cells) skeleton of fully continuous interparticle space.

The 2D scheme from Fig. 2a was replaced by two different points of view. One property from this pair must be determined from the particle set and the second from the properties of the chain. The first approach involves a comparison of the end-to-end length of the chain and the distance between the two closest particles (*Figure 2b*). The second approach involves a comparison of the chain volume and the volume of interparticle space (*Figure 2c*).

The length/distance approach investigates the interparticle distance. The cumulative distribution function of interparticle distances is an output of the AGLOMER software. The nearest particle distance (ND) is the distance between the two closest points on two spherical surfaces. The parameter ND is not a correct measure of distance between two surfaces. Therefore, it is useful to define some average

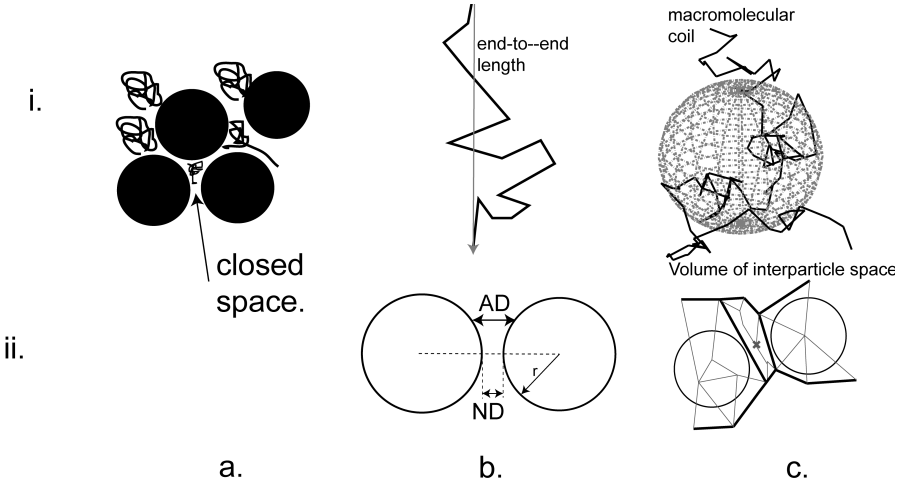

Figure 2: Perspectives on the statistical chain in the nano-particle system: (i) shape of chain – a. schematic approach, b. chain as a linear object having zero volume and a given length, c. a coil having a defined volume; (ii) properties related to the chain in the particle system - b. ND (nearest particle-particle distance), AD (average interparticle distance between two surfaces), c. Voronoi volume element of interparticle space.

distance between surfaces (AD). This is the average of the distances between two arbitrary points on two opposite spherical surfaces.

The mean end-to-end length, as a function of the number of segments, can also be calculated by *equation 1*.

The volume effect can be described by the Voronoi tessellation, which is described in detail in the next section. A comparative property to the Voronoi volume is the volume of a macromolecular coil. The volume is calculated from the mean end-to-end length.

Voronoi diagrams

The Voronoi diagrams can be constructed in an arbitrary set of n points. The principle of Voronoi analysis is the division of volume into a set of polyhedrons. One polyhedron is assigned to each of the points. The Voronoi cell is a convex polyhedron which ought to be complementary to other polyhedrons. The Voronoi diagrams used in this paper were calculated using the Qhull software [Barber, Dobkin

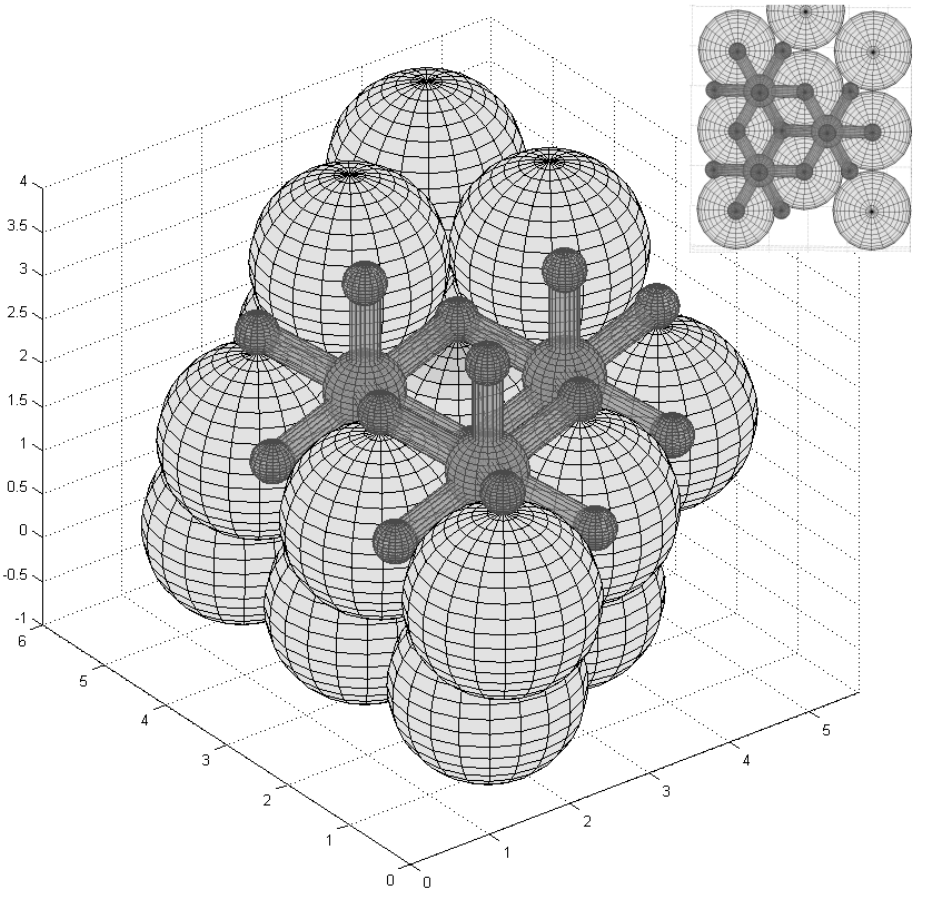

Figure 3: Hexagonal closest distribution of particles with a volume fraction of 74.04% of particles (light dark). The skeleton (dark phase) of the continuous matrix; in frame: xy-projection.

and Huhdanpa 1996] and implemented in a MATLAB environment.

2 Results and Discussion

The nano-composite system was represented by a set of particles. The set of particles was an output of the AGLOMER software and contained the matrix of relative coordinates and radii of 100,000 particles. The analysis was performed for a volume concentration of particles at 17.5%. This is the maximum limit of the con-

centration of particles in nano-composites but a common concentration in micro-composites. All the particle sets were generated with uniform particle size.

The size of particles was a free parameter of the model. The generated systems were analyzed in parallel. First, a system with a particle radius of 10 nm (nano-composites) was analyzed; second, a system with a particle radius of 1μm (micro-composite) was analyzed.

Chain length was a variable property of the model. The analysis was performed from three points of view: 1. the relationship between chain length and interparticle distance; 2. the relationship between chain volume and the interparticle space; and 3. the numerical models of chain and particles. The result of the analysis points to the presence of different structural elements in nano and micro-composites.

The first property which was analyzed on the particle set was the nearest particle distance. The nearest particle distances in a statistical set of particles were analyzed using the cumulative distribution function (CDF). The nearest particle distance (ND) was not an adequate property and had to be corrected. The average interparticle distance in the effective volume segment between two particles is higher than the nearest distance because ND is the distance between two spherical caps. The correction represents the average distance from an arbitrary point on the surface of one particle to another arbitrary point on the second particle. The situation is shown in *Figure 2* a. Two particles whose caps are almost in contact have a non-zero average distance between surfaces.

The nearest particle distance is shown in *Figure 4* as a *dotted curve*. From the dotted curve, it can be seen that 80% of the particles are very narrow (CDF at value x approaching zero). The nearest particle distance was corrected to the average distance between surfaces (AD). The cumulative distribution was then transformed to the *dash-dotted* curve in *Figure 4*. At this point, please ignore the following CDF curves of agglomerates (solid and dashed).

The above-mentioned graphs, valid for the interparticle distance in *Figure 4,* were drawn to the same graphs as properties of chains. The relation between end-to-end distance and the number of segments (*eq. 1)* was projected (lines on the right).The distance of the two nearest particles and the end-to-end lengths of chains were numerically compared. Therefore, both particle distance and end-to-end length on the x-axis were related to the particle radius. The cumulative distribution function of ND or AD can become a universal one for every particle size. However, the function of end-to-end length must be unique to every particle radius.

The correct function can be achieved by shifting up and down to the function belonging to the correct particle radius.

The current volume concentration of 17.5% is the maximum filling ratio of nano-

composites (15-20%), whereas micro-composites can be filled up to a volume of 50%. A part of the dash-dotted line (describing the average distance) in the graph is parallel to the y-axis (with an x-value approximately equaled to 0.1). This x-value (x = 0.1) divides the particle gaps (CDF = 0.8) into narrow gaps (about 80% of all gaps) and wide gaps (20%). The x value of the intersection of the *gray* line represents the chain length while the *dash-dotted* line represents distances between particles or the average chain length.

The number of segments in an average chain is marked in *Figure 4* by a gray arrow pointing to the right axis. The gap between microparticles (value 10 μm SP) is comparable to a chain containing 10^7 segments. There is a relatively thick polymer layer, which is enough for the separation of particles with volume fraction of 17.5%. A further increase in particle volume fraction is still possible. In the case where the particle size is reduced (10 nm SP), the average chain in the nano-particle gap has approximately 10 segments. The gap between 1 nm particles is even narrower than the one chain segment (the gray and dash-dotted lines do not intersect). Therefore, in a composite highly filled by nano-particles, agglomerates will be formed. When the agglomerates are formed in high amounts, the size of filler inclusions increases and the material loses its nano-composite character.

For further analysis, the particles in agglomerates were used instead of single particles. An agglomerate is a set of locally grouped particles. The definition of agglomerate is important. It is presumed that maximum parts of chains will be distributed in gaps between agglomerates. A particle is added to an agglomerate when its nearest distance to other particles in the agglomerate is closer than 10^{-4} of a radius. The nearest particle distance is replaced by the nearest distance of two particles from different agglomerates (*Figure 4-dashed*). As well as in particles, the nearest distance is not a relevant property. The mean distance between surfaces was analyzed (*Figure 4-solid*). Please ignore the CDF of particles (*dash-dotted* and *dotted* line).

Next, the curves of the distribution function were divided vertically. This is demonstrated in *Figure 4* by a *thin line* parallel to the y-axis where x is approximately equal to 1. Such a line divides the gaps between particles in agglomerates into two groups: gaps smaller than the x-value of the line (90% of gaps); and gaps larger than the x-value of the line (10% of gaps) (value CDF = 0.9). The intersection of the vertical line and lines representing the end-to-end lengths of a chain gives the number of chain segments. Such a chain is considered comparable to the size of gaps. Even if the nearest distance between two agglomerates is calculated (instead of the distance between particles), the nano-composite gaps are still small. They are comparable to the size of macromolecular chains of polymers either in nature or commonly used in technologies. In micro-composites, the gap is much larger than in common macromolecular chains.

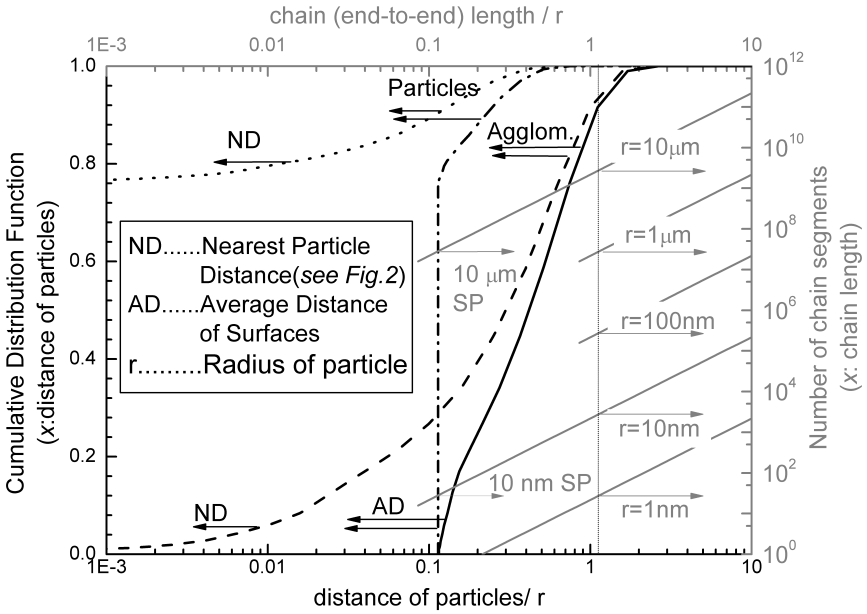

Figure 4: The cumulative distribution functions (CDF) of particle distance for single particles (dotted and dash-dotted) and particles from different agglomerates (solid and dashed); gray – function number of chain segments /end-to-end distance. The end-to-end distances are related to particle radius (radius of particle is the gray number under the arrow). Arrows point to numbers of chain segments where the chain is comparable to the gap between single particles (SP) or agglomerates.

Such an analysis has certain limitations. The chain is considered to be a linear object whereas in reality it has the characteristic shape of a worm-like chain. The AFM scan of a worm-like chain can be seen elsewhere [Akitaya, Seno, Nakai, Hazemoto, Murata and Yoshikawa 2007]. Besides, the comparison was limited to a certain segment of the volume between two particle surfaces. The volume segment, not directly between two surfaces, was excluded from the analysis. This is why the analysis produced a somewhat lower estimation of chain length than that which exists in reality.

Analysis of void interparticle volume

The next approach is complementary to the previous one (comparing particle distances/chain length). It is based on the characterization of interparticle spaces.

Interparticle spaces are large space cells which are bounded by several spherical surfaces. They can be compared to the size of a macromolecular coil. The most appropriate analysis for this purpose is the construction of Voronoi diagrams.

One random point outside the particles was generated. The Voronoi diagrams were constructed from this random point and the points of particle centers. Next, the facets of the random point's Voronoi cell were pushed out to the surface of the nearest particles. The volume of the element was then calculated. An example of a Voronoi cell of void space and the surrounding particles is shown in *Figure 5*. The dark polyhedron shows the Voronoi polyhedron of a random point. The surrounding light polyhedrons belong to the particles around this random point. In the figure, some light polyhedrons have been removed. In reality, the void cell is surrounded and hidden by the volume of other cells.

The analysis (the generation of a random point and the building of a Voronoi volume) was performed 10^6 times. Then, the statistical set of Voronoi volumes was analyzed by the cumulative distribution function.

The cumulative distribution function provides information about the statistical distribution of void space in the system. The statistical set of Voronoi volumes can be divided by a vertical line. The dotted vertical line in *Figure 6* divides the statistical set of volumes into volumes lower than the x-value of the vertical line (90% of volumes) and volumes higher than the x-value of the vertical line (10% of volumes) (value CDF = 0.9). The gray functions in *Figure 6* are the relation between the number of chain segments and the volume of a macromolecular chain. The volume of the macromolecular chain was calculated as a sphere with a radius equal to the end-to-end length. The function was related to the correct particle size (see comments re *Figure 4* in *Section 2.1* paragraph 3). The number of chain segments can be read from the intersection of the dashed vertical line and the gray functions in the graph. An adequate number of chain segments were read from the value on the right y-axis.

All the volumes found in the system are relatively large. Very small volume cells which cannot be filled by a chain are practically absent. This is in contrast to the particle distance distribution in *Figure 4*, where narrow gaps are very frequent. This can probably be explained in two ways. First, the random point probably hits larger space cells. Second, the volume elements most probably have an elliptical shape.

The comparison of Voronoi cells' volumes and macromolecular coil also has its limitations (like the previous comparison of distances and gaps). It assumes the spherical shape of a macromolecular chain. This, however, is not the case in reality.

Model of a real chain in the particle system

In contrast to previous methods, the following analysis does not depend on any

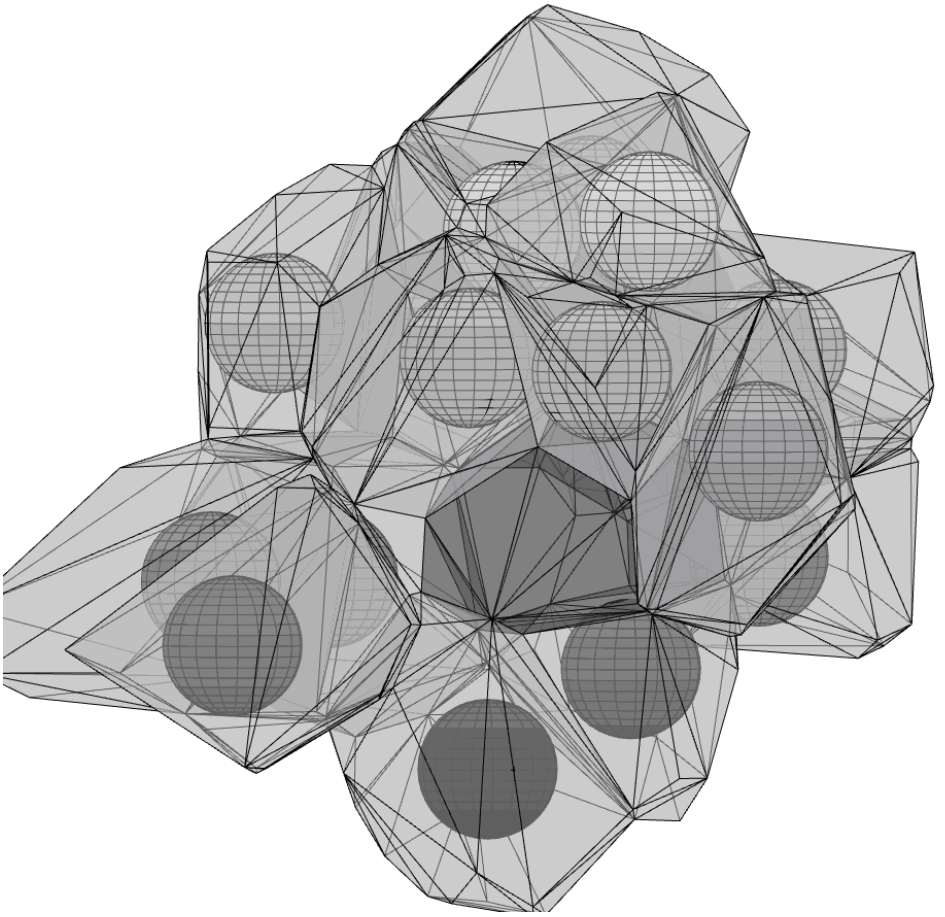

Figure 5: Voronoi diagrams of void space (dark gray) and particles (light gray). The dark cell is then inflated so that its facets are in contact with the particles.

point of view. However, it needs a sophisticated numerical tool for building a worm-like chain. It does not compare the distances but it qualitatively sorts the generated test chains.

The number of segments was an adjustable property of the chain's model. Each chain with a given number of segments was generated from the first segment to the last. The length of the segment was 0.153 nm (the length of the common carbon-carbon bond in the macromolecular backbone) and the so-called bond angle (see

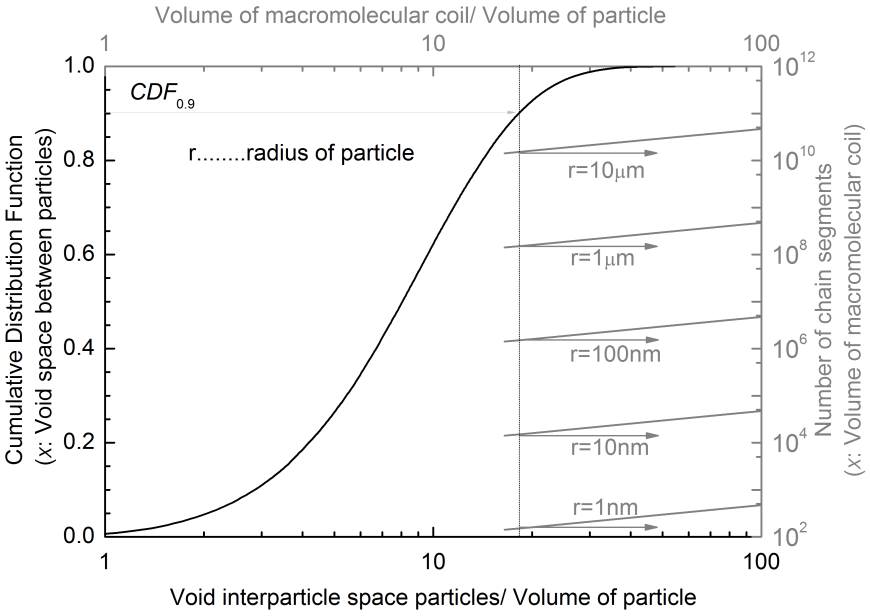

Figure 6: The cumulative distribution functions (CDF) of void spaces between particles calculated from the Voronoi diagrams; gray – relation between the number of chain segments and the volume of a macromolecular chain. The volume of the coil is related to the volume of the particle (the radius of the particle is the gray number under the arrow). Arrows point to the number of chain segments which forms a coil comparable to the void volume cells between single particles. (Analysis of agglomerates was not performed in this step).

Figure 1) was 110°. The chains were generated as freely rotating ones. This means that all the dihedral angles of segments were random numbers in the interval <0, 2π). In other words, the chain did not have preferred rotational states (trans and gauche) and all states were equally probable.

The chain was generated inside the set of particles. Its starting point was at a random point outside the particles. Every following segment had to avoid the particle and if an intersection was observed, its generation was repeated. However, each segment closer than 1nm to a particle surface was given the attribute of proximity together with the identification number of the particle.

The attributes of segment proximity to the particles were applied to the classifica-

tion of chains. Qualitative classes of chains (Φ, Ω and Ψ) were defined.

A proportion of chains contained only segments without attributes of proximity. Such chains, which are not in contact with any particles, are called free (F) and were associated in the class marked as Φ.

The next group of chains, marked as Ω, contained at least one segment with an attribute of particle proximity. They could have more segments with such an attribute but all segments had to be assigned to the same particle. An example of such a chain is the one that touches the particle at one point which leads to the formation of grafted chains (G). Eventually, it touches the particle with some adhered segments (A) or touches the particle with two distant segments while the chain between them is outside the zone of the particle. Then, the chain forms loops (L). Of course, the multiple presence of one component or different combinations of components (G, A, L) in one chain were frequently observed.

A special class of chains was called connectors (C). They comprised two distant segments that touch different particles. Chains containing at least one connector were associated with class Ψ.

The fractions of chains with no contact (Φ), in contact with a single particle (Ω), or in contact with two or more particles (Ψ) were analyzed for chains of different lengths. The fractions were calculated for a set of 10,000 chains. The relative positions of particles were identical. The difference was only found in particle radii. They were investigated in the case of nano-particles with a radius of 10 nm, and micro-particles with a radius of 1 μm. In both cases, the length of chain segment was identical. Therefore, the proportions of particle radius and chain segments were different for nano- and micro-composites.

A representation of the different classes is shown in *Figure 7*.

A very important result from the analysis is that while connectors are missing from micro-composites, they are present in nano-composites. This was presumed intuitively before the calculations (*Figure 1*). The numerical model of a worm-like chain can give more results which cannot be derived from previous analysis. In the case of micro-composites (r= 1 μm, ND single part= 0.10 μm, thickness of adhesion layer = 1 nm), chains which are directly influenced by particle surface are small in number (<0.1%). The properties of micro-composites will thus consist of independent contributions of particles, the matrix and geometry. The use of solid phase models is a good approximation. In the case of longer chains, the material contains a significant fraction of chains influenced by particles.

The situation in nano-composites (r= 10nm, ND agglom. part= 5 nm, thickness of adhesion layer = 1 nm) is more complicated. The shortest chains analyzed ($\approx$ 10 segments, length of segment = 0.153, bond angle 110°, with random dihedral angle,

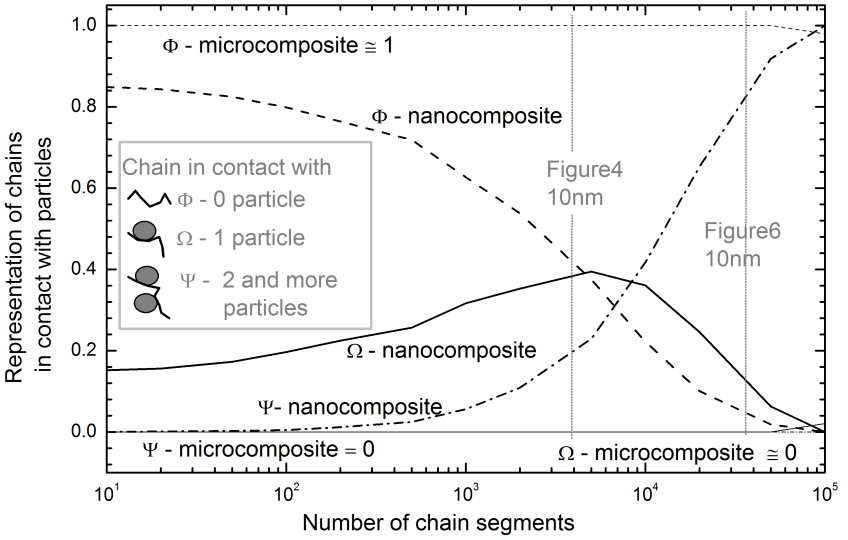

Figure 7: Distribution of selected types of chains as a function of molar mass of the chain in the case of nano-particles (10 nm diameter) and micro-particles (1 μm diameter); Φ - free chains having no contact with particles; Ω - chains in contact with one particle; Ψ - chains connecting two or more particles; thick-nano-composite; thin-micro-composite

i.e. the chains did not have preferred trans and gauche positions) were short for the connection of particles. Connectors were not observed. However, a significant proportion of chains (about 15%) interacted with one particle. If such an effect plays a role, the effect of the nano-particle must also be observed in wax. This was observed experimentally. For example, the addition of a nano-filler increases the viscosity of paraffin wax even at a concentration of 2% [Wang, Calhoun and Severtson 2008]. The effect can be visible in some properties such as elongation at break, creep, or yield strength.

In the middle length region, from 1,000 to 10,000 segments, the fraction of chains influenced by particle surfaces increases and, at the same time, the number of chains connecting two particles increases while the number of free chains decreases.

The longest chains (>10,000 segments) form with nano-particles an infinite network in which nano-particles act as the nodes. The consequence of such a structure

for macroscopic properties is a certain limit on macromolecular weight. Above the limit, macroscopic properties are unaffected by of increasing molecular weight [Fornes, Yoon, Keskkula and Paul 2001]. In particular, properties like yield strength or elongation at break are independent of molecular weight when some limiting value is exceeded. All properties that are independent of molecular weight have a common attribute. They are particularly driven by the dynamic behavior of macromolecules on the particle's surface.

Finally, the results from the combined models of chain and particles should be compared with the results in *Figures 4 and 6*. For nano-composites, the transition between macromolecules showing the gelation of structure is about 10^3 segment chains. As was expected, the results from the numerical model of a worm-like chain and particles are between the lowest estimation (calculated from a comparison of gaps between particles and chain length) and the highest estimation (calculated from a comparison of interparticle volume and volume of chain). Therefore, the last model (the combination of real numerical worm-like chains and models of nanoparticles) improves upon the analysis of the two previous approaches.

Like the two previous models, this model also has limitations. Real polymer has several attributes which are missing from the model. It presents a static snapshot of the chain inside the particles. However, the chain is, in reality, moving. Therefore, dynamic properties must be applied in the future.

3 Conclusion

The distribution of void interparticle space is an important factor in the study of nano-composites. It influences the structural factors that can be used for the interpretation of macroscopic properties. For the most part, interpretations are based on 2D schematic pictures. Such schematic models may lead to misinterpretation of structure-property relations. The 3D model reveals some structural features that are frequently absent in 2D schemes. One example of such features is space cells enclosed by particles. They are common in 2D models but completely absent from 3D models, even with high volume fillings of particles.

A model of particles in a volume fraction of 17.5% was investigated. While this is the maximum volume fraction used in nano-composites, it is a common volume fraction for micro-composites. The 3D space filled by particles can be analyzed statistically. The nearest interparticle distance was compared with the mean end-to-end length. The volume cells among particles are relatively large in comparison with the size of chains that are commonly used in experimental nano-composite systems (approximately 1,000 segments). The same results were found when combining worm-like chains and particles. Connectors of two particles were observed

in chains that are much longer.

There is probably still another factor that accounts for the existence of specific nano-composite properties. However, the geometrical restriction of chains is not sufficient to be the cause.

Acknowledgement: A financial support through Specific Research Grant of Brno University of Technology No. FAST/FCH/FSI-S-11-1 is acknowledged. This research was also supported by the Ministry of Education of the Czech Republic under research project MSM 0021630501.

References

Agarwall, B.D. (1972): Micromechanics Analysis of Composite Materials Using Finite Element Method, *PhD thesis,* University Microfilms International, Michigan USA.

Akcora, P.; Liu, H.; Kumar, S.K. ; Moll, J.; Li, Y.; Benicewicz, B.C.; Schadler, L.S.; Acehin, D.; Panagiotopoulos, A.Z.; Pryamitsyn, V.; Ganesan, V.; Ilavsky, J.; Thiyagarajan, P.; Colby, R.H.; Douglas, J.F. (2009) : Anisotropic self-assembly of spherical polymer-grafted nanoparticles, *Nature Materials* vol. 8, no. 4, pp. 354-359.

Akitaya, T.; Seno, A.; Nakai, T.; Hazemoto, N.; Murata, S.; Yoshikawa, K (2007): Weak Interaction Induces an ON/OFF Switch, whereas Strong Interaction Causes Gradual Change: Folding Transition of a Long Duplex DNA Chain by Poly-L-lysine", *Biomacromolecules,* vol. 8, no. 1, pp. 273-278.

Bansal, A.; Yang, H.C.; Li, C.Z.; Cho, K.W.; Benicewicz, B.C.; Kumar, S.K.; Schadler, L.S. (2005) : Quantitative Equivalence Between Polymer Nanocomposites and Thin Polymer Films, *Nature Materials,* vol. 4, pp. 693-698.

Barber, C.B.; Dobkin, D.P.; Huhdanpa, H.T. (1996) : The Quickhull algorithm for convex hulls. *ACM Trans. on Mathematical Software*,vol. 22, pp. 469-483.

Bizet, S.; Galy, J.; Gérard, J.F. (2006): Molecular dynamics simulation of organic–inorganic copolymers based on methacryl-POSS and methyl methacrylate, *Polymer,* vol. 47, no. 24., pp. 8219-8227.

Fornes, T.D.; Yoon, P.J.; Keskkula, H.; Paul, D.R. (2001): Nylon 6 nanocomposites: the effect of matrix molecular weight, *Polymer*, vol. 42, no. 25, pp. 9929-9940.

Hynstova, K.; Jancar, J.; Zidek, J. (2006): Molecular Dynamics Simulation of Single Chain in the Vicinity of Nanoparticle, *Key Engineering Materials*, vol. 334-335, pp. 373 - 376.

Jancar, J.; Douglas, J.F.; Starr, F.W.; Kumar, S.K.; Cassagnau, P.; Lesser, A.J.; Sternstein, S.S.; Buehler, M.J. (2010): Current issues in research on structure–property relationships in polymer nanocomposites. *Polymer*. vol. 51, no. 15, pp. 3321-3343.

Kalfus, J.; Jancar, J. (2007): Elastic response of nanocomposite poly(vinylacetate)-hydroxyapatite with varying particle shape. *Polymer Composites,* vol 28, no. 6, pp. 365 – 371.

Knauert, S.T.; Douglas, J.F.; Starr, F.W. (2007): The Effect of Nanoparticle Shape on Polymer-Nanocomposite Rheology and Tensile Strength. *Journal of Polymer Science Part B: Polymer Physics*, vol. 45, no. 14, pp.1882–1897.

Osman, M.A.; Atallah, A. (2004) : High-Density Polyethylene Micro- and Nanocomposites: Effect of Particle Shape, Size and Surface Treatment on Polymer Crystallinity and Gas Permeability. *Macromolecular Rapid Communications*, vol. 25, no. 17, pp. 1540 – 1544.

Torquato, S.; Hyun, S.; Donev, A. (2002) : Multifunctional Composites: Optimizing Microstructures for Simultaneous Transport of Heat and Electricity. *Physical Review Letters*, vol. 89, no. 26, pp. 266601-1-266601-4.

Wang, J.; Calhoun, M.D.; Severtson, S.J. (2008): Dynamic Rheological Study of Paraffin Wax and Its Organoclay Nanocomposites. *Journal of Applied Polymer Science*, vol. 108, no. 4, pp. 2564–2570.

Ye, L.; Lai, Z.; Liu, J.; Tholen, A. (1999): Effect of Ag Particle Size on Electrical Conductivity of Isotropically Conductive Adhesives. *IEEE Transactions on Electronics Packaging Manufacturing*, vol. 22, no. 4, pp. 299-302.

Zidek, J.; Kucera, J.; Jancar, J. (2010): Model of Random Spatial Packing of Rigid Spheres with Controlled Macroscopic Homogenity. *CMC: Computers, Materials & Continua*, 16, no.1, pp. 1-23.